Oil & Natural Gas Technology

DOE Award No.: DE-FE0028895

Quarterly Research Performance Progress Report (Period ending 6/30/2017)

Dynamic Behavior of Natural Seep Vents: Analysis of Field and Laboratory Observations and Modeling

Project Period (10/01/2016 to 09/30/2017)

Submitted by:
Scott A. Socolofsky

Texas A&M Engineering Experiment Station
DUNS #:847205572.
3136 TAMU
College Station, TX 77843-3136
e-mail: socolofs@tamu.edu
Phone number: (979) 845-4517

Prepared for:
United States Department of Energy
National Energy Technology Laboratory

July 31, 2017

U.S. DEPARTMENT OF ENERGY | NATIONAL ENERGY TECHNOLOGY LABORATORY

Office of Fossil Energy

DISCLAIMER:

Contents

List of Figures

List of Tables

1 Accomplishments

1.1 Summary of Progress Toward Project Objectives

The *overarching goal* of this project is to develop a computer model to predict the trajectory and dissolution of hydrate-armored methane bubbles originating from natural seeps. The model is based on the Texas A&M Oilspill (Outfall) Calculator (TAMOC), developed by Dr. Socolofsky, and which will be refined and validated through this project to explain fundamental laboratory and field observation of methane bubbles within the gas hydrate stability zone of the ocean water column. *Our approach* is to synthesize fundamental observations from the National Energy Technology Laboratory's (NETL) High-Pressure Water Tunnel (HPWT) and field observations from the Gulf Integrated Spill Research (GISR) seep cruises (cruises G07 and G08), conducted by the PIs in the Gulf of Mexico, to determine the dissolution pathways and mass transfer rates of natural gas bubbles dissolving in the deep ocean water column. We will achieve these objectives by pursuing the *following specific objectives*:

1. Analyze existing data from the NETL HPWT.
2. Synthesize data from the GISR natural seep cruises.
3. Refine and validate the seep model to predict available data.
4. Demonstrate the capability of the seep model to interpret multibeam data.

Ultimately, the *main outcome and benefit* of this work will be to clarify the processes by which hydrate-coated methane bubbles rise and dissolve into the ocean water column, which is important to predict the fate of methane in the water column, to understand the global carbon cycle, and to understand how gas hydrate deposits are maintained and evolve within geologic and oceanic systems, both at present baselines and under climate-driven warming.

The work accomplished during this reporting period focused on the first two specific objectives. For the NETL HPWT data, we have developed a procedure for evaluating the hydrate formation time in the experiments, have organized the high-speed video imagery for tracking hydrate crystals on the bubble-water interface, and have validated our bubble size determination methods with data in the NETL reports. We have further used the bubble shrink rate data to compute the mass transfer coefficient, the main parameter for bubble shrinkage in the TAMOC model. For the GISR field data, we have completed all of the data analysis from the high-speed camera and are in the

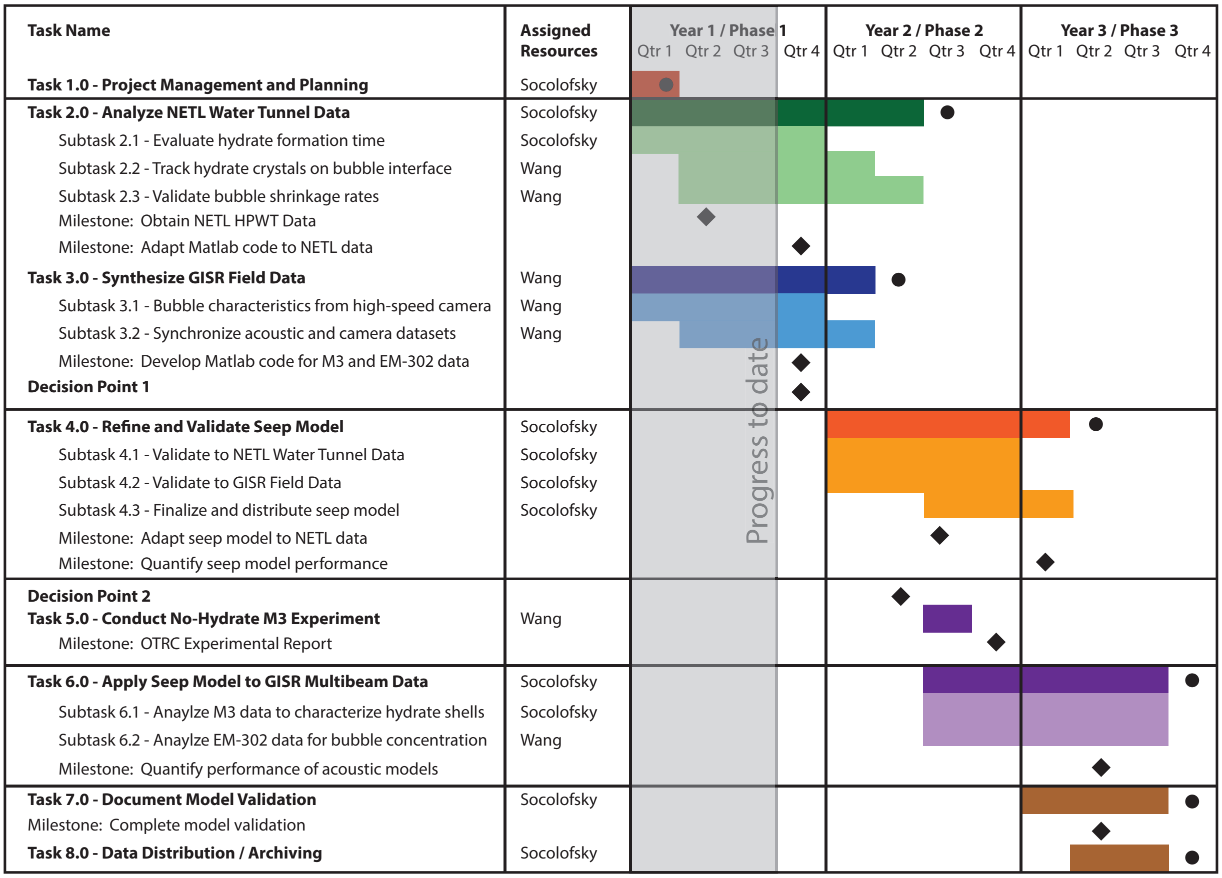

Figure 1: Project Timeline.

process of refining our acoustic algorithms for obtaining quantitative information from the M3 and EM-302 echo sounders used during the GISR cruises. We are currently collating the analysis data and preparing documentation for Decision Point 1 (see § 1.2.4) and Milestones 2 and 3 (see § 1.4). Based on the progress during this quarter, the project is currently on schedule.

1.2 Progress on Research Tasks

Figure 1 presents the project timeline, showing each of the project tasks, subtasks, and milestones as identified in the Project Management Plan (PMP). The present reporting period concludes the third quarter of FY 2017 (Phase 1 of the project). During this period, we made progress on each subtask of Tasks 2 and 3 leading up to Decision Point 1, which is due in the next quarter. The work conducted on these tasks during this reporting period is summarized in the following sections, organized by each Task.

1.2.1 Task 1.0: Project Management Planning

The Project Management Plan was completed during the first quarter of Phase 1 and accepted in final form as of October 28, 2016.

1.2.2 Task 2.0: Analyze NETL Water Tunnel Data

In this project, we will analyze the comprehensive data set of HPWT data collected by NETL. To do this, we have transfered a complete copy of all raw data (primarily image files and time history data of pressure and temperature in the HPWT during each experiment) to Texas A&M University and have installed this data on a secure internal server. Data transfer was completed on March 24, 2017, and achieved Milestone 1 for the project (Obtain NETL HPWT Data). The sections below summarize our progress during the present reporting period in analyzing this data.

Subtask 2.1 - Evaluate Hydrate Formation Time

The complete set of image data for the HPWT experiments allows an analysis of the kinetics of hydrate formation on methane bubbles under different pressure, temperature, and dissolved methane conditions during free rise of a bubble in the water column. In our Phase 1, 2nd Quarter Progress Report, we outlined a detailed procedure for identifying important events during each HPWT experiment, including the onset of hydrate forming conditions, the point at which a complete hydrate shell is formed, transition out of the hydrate stability zone (HSZ), the dissociation period, and complete dissociation of formed hydrate outside the HSZ. During the present reporting period we have been analyzing video data from the HPWT archive and applying this methodology to record hydrate formation times. This data analysis is ongoing, and no new results are yet available to report during the present reporting period.

We have identified one challenge in getting exact values for hydrate formation time for all experiments. Bubbles were released into the HPWT as follows: a small orifice injector released a metered amount of methane gas into the water tunnel, this gas rose into an inverted cup that captured the gas, to release the gas into the counterflow, the cup is rotated through 180°, and the bubble then rises up through the inverted cone counterflow device to the viewing section. The image data accurately record the moment that the bubble enters the viewing section. However, the elapsed time during which the bubble is resident in the inverted cup before it is released is not reported. In the journal paper by Warzinski et al. (2014) it is reported that the bubble analyzed in that paper was released after 257 s. Based on their Figure 1, is appears that the bubble was released at the same time that the pressure was increased to 10 MPa. However, the pressure while the bubble was in the cup was about 6.6 MPa; hence, this time is not negligible for calculating the hydrate formation time.

We will discuss the question of whether or not a record of the resident time for each bubble in the release cup is available with Franklin Schaffer at NETL and compare the time history data for pressure and temperature in the data archive with the video data to determine whether or not this time in the cup can be identified. If this time can be determined, then it will be possible to determine hydrate formation times for all bubbles tested in the HPWT. In most experiments, hydrates were formed, dissociated, and reformed. For all reformation stages, the exact moment that the HSZ is crossed is known from the temperature and pressure history; thus, it will be possible to have precise hydrate formation times for all subsequent armoring of bubbles during prolonged experiments.

At the present time, this unknown residence time in the release cup is not delaying progress as we are continuing to evaluate the video data to determine hydrate armor characteristics following the procedure outlined in our previous Progress Report. Subtask 2.1 is scheduled to be completed in the next reporting cycle, and the database of hydrate formation times is part of the content of the success criteria for Decision Point 1. This task is on schedule, and we expect to have the complete database of hydrate formation times based on the imagery time stamps by the end of Phase 1, as planned in the timeline in Figure 1.

Subtask 2.2 - Track Hydrate Crystals on Bubble Interface

Two types of image data were collected in the HPWT experiments. One camera recorded at a relatively low frame rate (about 15 fps) and recorded continuously for the entire duration of the experiment. A second camera recorded at high frame rates (up to 1000 fps), but could only record short time sequences (order a few seconds). After a short image sequence was collected, the data had to be downloaded from the camera before another image sequence could be collected. Hence, there are a few high-speed image sequences collected per each experiment, with at least 5 minutes between high-speed image burst. Also, it appears that the high-speed camera did not exist during the early experiments so that high-speed image data are only available for a subset of the complete experimental matrix.

To track the motion of hydrate crystals on the bubble-water interface, only the high-speed data can be used. Through communications with Franklin Shaffer at NETL, he shared several videos

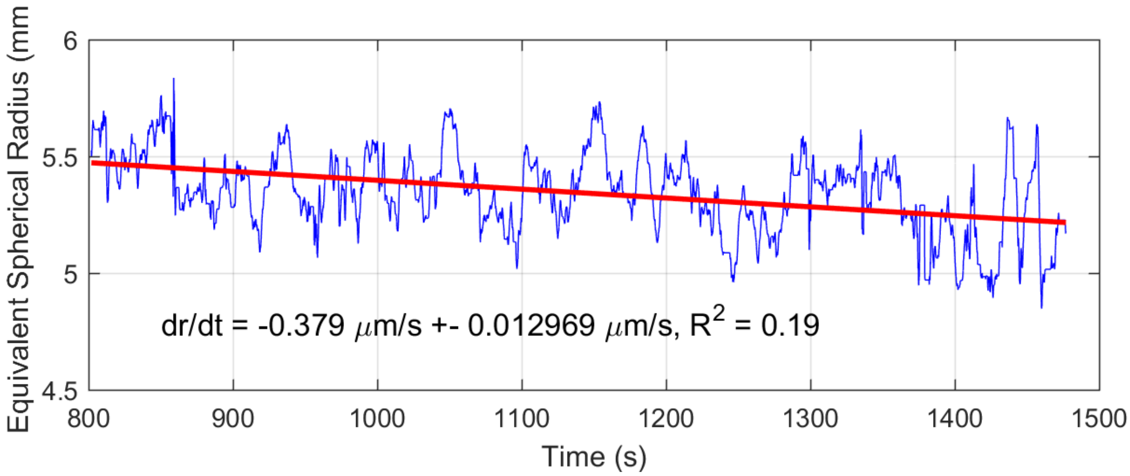

Figure 2: Equivalent spherical radius for image data processed for the 3rd bubble on June 11, 2012 during time sub-set 802 s to 1477 s: blue line is the evaluated value from the image data; red line is a best-fit line for the shrinkage rate.

clips they had analyzed to determine the fractional area of coverage by hydrate during the period where hydrate has not yet covered the whole bubble. By watching these videos, it is clear that the hydrate crystals in some of the high-speed images are moving and can be tracked. We have identified the raw data for these image sequences, and we will begin tracking hydrate crystals from these data in the next two performance periods, as planned in the timeline in Figure 1.

Subtask 2.3 - Validate Bubble Shrinkage Rates

Bubble size and shape can be evaluated from both the slow-speed and high-speed data. The slow-speed data are used to determine the overall shrinkage rate of the bubbles due to dissolution, and the high-speed data can be used to understand the time scales of bubble oscillations and rotations. A sample analysis result from both of these datasets was reported in our Phase 1, 2nd Quarter Progress Report. During the present reporting period, we have been using our validated image processing code to evaluate bubble shrinkage rates and have begun analyzing the bubble shrinkage rate data to calculate mass transfer coefficients.

Evaluate Bubble Shrinkage Rate. During the present reporting period, we have applied our image processing code to evaluate bubble sizes for much of the HPWT image data. In Figure 2, we provide one example for the third bubble released on June 11, 2012 during imaging times from 802 s to 1477 s. This plot corresponds to a similar plot in the NETL report, Appendix C (Levine et al. 2015), and is for nearly constant ambient conditions. The exact temperature and pressure history during this experiment has also been extracted from the HPWT dataset, and is shown in

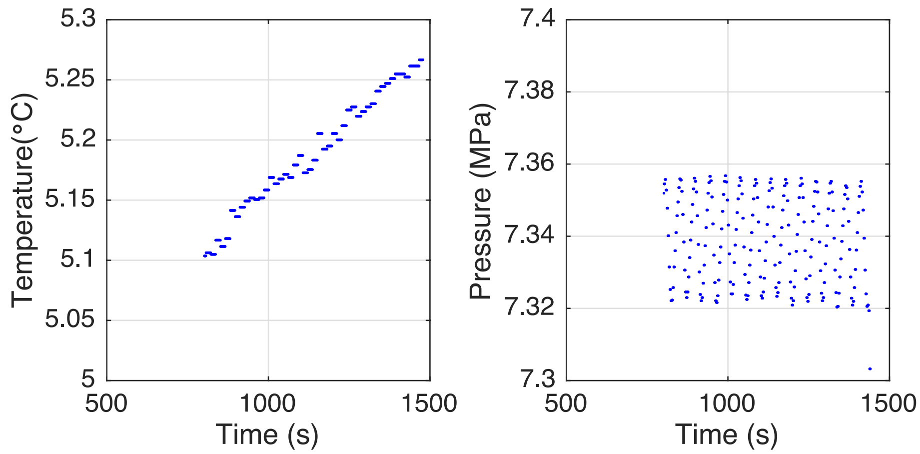

Figure 3: Temperature (left) and pressure (right) variation in the HPWT during the experiment depicted in Figure 2.

Figure 3. These figures are very similar to those in the NETL report (Levine et al. 2015) and validate our image processing and data extraction methods.

The bubble size data in Figure 2 is also typical of data for bubble shrinkage in the HSZ. The total duration of the image sequence is 675 s (11.25 min), and the oscillations in the bubble size due to viewing the oblate object from different angles as it wobbles (peak-to-peak excursions of the blue line in Figure 2) cover the range from 5.3 to 5.7 mm equivalent spherical radius throughout the measurement period. Indeed, the shrink rate is low (-0.4 μm/s), and the correlation coefficient r^2 for the best-fit line is correspondingly low (in this case, 0.19). Although the reported uncertainty in the shrink rate ($\pm$0.01 μm/s) represents a low relative error of only 3%, this is a misleading statistic for the goodness-of-fit of this shrink-rate line, and we are consulting the statistics literature to determine the true uncertainty in the shrink rate.

Progress on this sub-task is on schedule (refer to Figure 1), and evaluation of the shrink rate data for all images in the HPWT dataset is ongoing. Although our image processing algorithms validate the shrink rate data reported in the NETL reports (Levine et al. 2015), we are reanalyzing the data in order to compute the uncertainty in the shrink rates using different statistics (ongoing for the next reporting period). We will use this quantitative uncertainty to estimate the uncertainty of the mass transfer coefficient, as explained in the next paragraph.

Calculate Mass Transfer Coefficient. Computer models for bubble evolution predict dissolution from bubbles using the mass transfer coefficient, an empirical parameter that relates the mass loss rate from the bubble to a chemical potential across the bubble-water interface. The typical form of the mass transer equation is

$$\frac{dm_i}{dt} = -A\beta_i(C_{s,i} - C_i) \tag{1}$$

where m_i is the mass of constituent i inside the bubble, A is the surface area of the bubble, β_i is the mass transfer coefficient (dimensions of L/T) for constituent i, $C_{s.i}$ is the solubility of constituent i in the surrounding fluid (here, water) and C_i is the concentration of constituent i dissolved in the surrounding fluid. The mass transfer coefficient combines both the physical characteristics of the turbulent boundary layer around the bubble and the chemical properties of the molecular diffusion of constituent i into a single mass transfer parameter β_i. Existing correlations for β have been reported in Clift et al. (1978), and relate the Sherwood number $Sh = \beta d_e/D$ to the hydrodynamic state of the bubble (e.g., Reynolds number), where d_e is the equivalent spherical diameter of the bubble and D is the molecular diffusion coefficient.

During the present reporting period, we have used Eq. 1 with the measured shrinkage rates to compute β_i for methane from the measured data. The mass m and volume V of a bubble are related by $V = m/\rho_p$, where ρ_p is the density of the fluid in the bubble. Throughout this discussion, we use the subscript p to denote the gas phase, and we drop the subscript i since we will focus only on the experiments with pure methane (single-constituent bubbles). At constant temperature and pressure, ρ_p is constant. Taking $V = 4\pi r_e^3/3$ and $A = 4\pi r_e^2$, we can rewrite Eq. 1 as

$$\frac{dr_e}{dt} = -\frac{\beta}{\rho_p}(C_s - C) \tag{2}$$

where r_e is the radius of an equivalent sphere having the same volume as a given bubble. Solving for the mass transfer coefficient, we have the following equation

$$\beta = -\frac{\rho_p}{\Delta C}\frac{dr_e}{dt} \tag{3}$$

where ΔC is $(C_s - C)$, and the right-hand-side contains quantities either measured during the experiments (dr_e/dt and C) or computable from an equation of state using the measured thermodynamics conditions (ρ_p and C_s, which depend on temperature, pressure, and salinity of the ambient water).

There are two main questions we are trying to answer using the β values computed from Eq. 3. First, there is the open question regarding what is actually dissolving. The possible answers are 1.) the free gas inside the bubbles, 2.) the hydrate shell itself, or 3.) a combination of both the free gas and the hydrate shell. Second, it is unknown whether the mass transfer coefficient will take on known values, such as those reported in Clift et al. (1978), or slower mass transfer rates, owing to the hydrate armoring.

To answer the first question, we compare computed values of β for different values of C_s, taking C_s as either the solubility of the gas phase or the hydrate phase. To operate the experiments, NETL already determined the solubility of the hydrate phase, and we use their equation for hydrate solubility in our analyses. For pure methane solubility and for gas density, TAMOC includes the required equations of state.

For the second question, we can compare calculated values of β for different choices of C_s with values computed from correlation equations in Clift et al. (1978). There are two types of correlations: those for clean bubbles and those for dirty bubbles. Clean bubbles have a mobile gas/water interface and are rarely observed in nature; dirty bubbles have a rigid gas/water interface (non-circulating). Bubble/water interfaces can be rigid either due to a hydrate shell or as a result of Marangoni forces that develop on the bubble/water interface due to gradients in the concentration of naturally occurring surfactants that attach to the gas/water interface. We would expect mass transfer rates that are either equivalent to or slower than dirty bubble rates for hydrate armored bubbles, and we expect mass transfer rates equivalent to dirty bubbles for pure methane bubbles outside the HSZ as long as they have no hydrate crystals on the gas/water interface. We may expect to find clean bubble mass transfer rates during the hydrate formation and dissociation phase when hydrate plates are moving on the bubble/water interface, and this is the reason we will be tracking hydrate crystals on the gas/water interface in Subtask 2.2.

To compare the computed mass transfer rates from Eq. 3 to known correlations, we should carefully propagate the experimental error. The normal error propagation formula uses a root-mean-square error, and is given in this case by

$$\delta\beta = \sqrt{\left(\frac{-1}{\Delta C}\frac{dr_e}{dt}\delta\rho_p\right)^2 + \left(\frac{\rho_p}{\Delta C^2}\frac{dr_e}{dt}\delta\Delta C\right)^2 + \left(\frac{-\rho_p}{\Delta C}\delta(dr_e/dt)\right)^2} \tag{4}$$

where δ is an operator indicating the error in the following quantity. Errors in the gas density from the equation of state ($\delta\rho_p$) are in the range of $\pm 3\%$. The error in the background gas concentration δC depends on the accuracy of the gas metering pump and the amount of gas in the background water, which can be computed from the information in the NETL reports. Errors in the hydrate solubility are between 5% and 10%, depending on the distance from the HSZ and the salinity. Finally, the error in the shrinkage rate ($\delta(dr_e/dt)$) is given by the uncertainty in the linear slope for the fitted line in Figure 3.

We are currently in the process of evaluating each of these errors and computing error bounds for the computed mass transfer coefficients for each experiment. This analysis yields a matrix of four possibilities: clean or dirty mass transfer rates with ΔC computed from methane or hydrate solubility. Preliminary results support dirty bubble mass transfer rates for hydrate free and hydrate armored bubbles with ΔC based on the free gas solubility. This work is ongoing, and will continue into the next reporting period. Knowing the correct form of ΔC and the relationship between the computed β in the experiments to known correlations for clean and dirty bubbles is a necessary step to adapt and validate the TAMOC model in Task 4.0, which will begin in Phase 2. Hence, Task 2.0 remains on schedule and is providing important data on the general behavior of methane bubbles under deep ocean conditions and data needed for model development.

Progress Toward Milestones

Milestone 1 (Obtain NETL HPWT Data) was completed on March 24, 2017. The other major milestone for Task 2 is to adapt our image analysis codes in Matlab to analyze the image data in the HPWT Dataset. This has been completed, and a brief report demonstrating the success of our analysis code is due in the next reporting period. We are on schedule to complete this milestone (see § 1.4).

1.2.3 Task 3.0: Synthesize GISR Field Data

The project PIs conducted two research cruises to natural seeps in the Gulf of Mexico under funding to the GISR consortium. These were the G07 cruise in July 2014 to Mississippi Canyon (MC) block 118 and to Green Canyon (GC) block 600 and the G08 cruise in April 2015 to MC 118. Both cruises were on the *E/V Nautilus* and utilized the remotely operated vehicle (ROV) *Hercules*. This project utilizes two main datasets from these cruises: data from our stereoscopic high-speed camera system mounted on the ROV (Wang et al. 2015) and acoustic data collected by an M3 sonar mounted on the ROV and an EM-302 multibeam sonar mounted on the haul of the ship. The image data from the G07 cruise was analyzed previously and reported in Wang et al. (2016). This project will analyze all of the acoustic data and complete analysis of the image data for the G08 cruise. The sections below summarize our progress during the present reporting period in analyzing this field data.

Subtask 3.1 - Bubble Characteristics from High-Speed Camera.

All of the GISR imaging data analysis is now completed. In our first Progress Reports, we have shown several results of this analysis. The complete dataset includes the bubble size distribution, rise velocity of bubbles, volume flux of the bubble from each vent, and shrinkage of the bubbles over 400 m height-of-rise. We are currently formatting this data into an Excel database that will be transfered to NETL as part of Decision Point 1 (see § 1.2.4).

Subtask 3.2 - Synchronize Acoustic and Camera Datasets.

Data Synchronization. Synchronization between the two sets of acoustic data (M3 and EM-302) and the imaging data is now completed. This includes the synchronization of 1.) camera measurements at the seep source and in the plume at different altitudes with data from the M3 acoustic profiling experiment, and 2.) camera measurement at the seep source and in the plume at different altitude synchronized with the EM-302 water column profiling of the bubble backscatter.

The synchronization Set 1 will be used to build the seep bubble dissolution model and random walk diffusion model using the imaging data as input, which predicts the bubble properties in the water column. The modeled evolving bubble properties (size distribution, spreading of the bubbles) will be used to create the acoustic maps at different altitudes, which will be compared to the M3 sonar data. This synchronization is expected to help with further analysis of the M3 sonar data. One ongoing task is to obtain the bubble size distribution or volume flux using the M3 sonar and an acoustic model. The synchronized camera data will be used as reference to calibrate the acoustic model of the sonar measurements.

The synchronization Set 2 enables comparison of the rise height of bubble flares from the sea floor between *in situ* observations and estimates from the water column data from the haul-mounted EM-302. Since the EM-302 surveys occurred during the turn-over time of the ROV, synchronization in this case refers to the match of each dive at each seep site between camera measurements and subsequent EM-302 sonar measurements. The measurement of bubble size distribution and volume flux will be used to build seep bubble dissolution model. The modeled evolving bubble parameters will be used to calculate the profile of target strength of the bubble backscattering, which will be compared to the EM-302 data.

Acoustic Modeling. GISR cruises G07 and G08 acquired uncalibrated backscatter amplitude of the seep bubbles from the EM-302 at 30 kHz acoustic signal. The backscatter amplitude is the true echo level adjusted by the sonar system with amplification using range-dependent TVG (Time Varying Gain). All of the system parameters are recorded in the water column datagram so the conversion from backscatter amplitude to echo level can be performed. The target strength of the seep bubbles can therefore be calculated from the echo level using the sonar equation. However, since the sonar system is uncalibrated, it is not possible to obtain the true target strength of the seep bubbles. Despite this limitation, we expect the profile of uncalibrated target strength still represents the quantitative evolving feature of seep bubbles, and we have demonstrated the similarity of these profiles in our previous progress reports. Thus, the EM-302 sonar data is valuable to compare with model results (setting up Task 4.0).

GISR cruises G07 and G08 also used a forward-looking M3 sonar to measure the cross section of seep bubble plumes at different heights in the water column. Similar to the EM-302, the M3 sonar was used as an uncalibrated system during our field experiment. A variety of factors affect the final intensity of the acoustic measurement. The sonar range has been changed from time to time during the experiment, therefore, the power of transmitted pulse is different and the transmission loss is a function of the range. Also, when the sonar range increased, some bubbles may be smaller than the sonar resolution and become an extended target, which is treated differently from a point target. We have consulted the technical support from the manufacturer of the M3 (Kongsberg) and concluded that with an uncalibrated system, it may not be feasible to obtain the bubble characteristics from the M3 sonar data without direct comparison between uncalibrated and calibrated systems. This is the purpose of Task 5.0, the M3 experiment in the OTRC, scheduled in Phase 2.

Progress Toward Milestone

The major milestone for Task 3 is to create a Matlab analysis program that can use the TAMOC model together with the acoustic data to infer bubble properties for bubbles observed in the acoustics. Our approach follows an approach by Weber et al. (2014), and we have continued to develop our analysis code during the present reporting cycle, where we have focused on developing accurate measures of target strength and have studied the differences between our uncalibrated data and the type of data that can be obtained from a calibrated acoustic system. This work for Task 3.0 is now complete, and we are working on a brief report for Milestone 3, due in the next reporting period.

1.2.4 Decision Point 1

As detailed in the PMP, Decision Point 1, scheduled for the end of Phase 1 has the following two go/no go success criteria:

- Subtask 2.1 (Evaluate hydrate formation time) should be completed in Phase 1. The recipient shall provide to DOE a table of data listing each HPWT experiment and the hydrate formation time evaluated for that experiment. For experiments where the hydrate formation time cannot be evaluated, a comments column shall be included with the table explaining the reason. The completed data table shall demonstrate success of this criterion.

- Subtask 3.1 (Bubble characteristics from high-speed camera) should also be completed in Phase 1. The recipient shall provide to DOE a second table of data listing each high-speed camera dataset for both the 2014 and 2015 GISR cruises and the post-processed values of the median bubble diameter, the standard deviation of a log-normal fit to the volume size distribution, and the mean rise velocity of the bubbles. The completed data table shall demonstrate success of this criterion.

As detailed above, we have completed the methodology for Subtask 2.1 and are currently evaluating the video data to extract the hydrate formation times. We have also completed all of the data analysis for Subtask 3.1. During the next reporting period, we will compile the required data tables and submit them to NETL before September 30, 2017. We are currently on schedule to complete these two success criteria, thus passing Decision Point 1.

1.3 Deliverables

To date, we have completed the following list of deliverables:

1. **Project Management Plan (PMP)**. The PMP was delivered in its accepted and final form on October 28, 2016.

2. **Data Management Plan (DMP)**. No revisions were requested by the Project Officer to the plan submitted with the proposal; hence, the original DMP is the present guiding document. Revisions will be updated as necessary throughout the project as required by the Project Officer.

In the present reporting period, no new deliverables were due. The next set of deliverables include complete archives of the analysis data produced through analysis of the HPWT and GISR Seep Cruise data. Progress toward these deliverables is summarized above in the reporting for each Task.

1.4 Milestones Log

Table 1 presents the schedule of milestones with their verification methods for the duration of the project period. Milestone 1 was completed on time. Milestones 2 and 3 are due in the next reporting period. See Section 1.2 for details on progress toward completion of these up-coming milestones, which are proceeding on schedule.

1.5 Plans for the Next Reporting Period

Work for the next reporting period will continue on Tasks 2 and 3 (refer to Figure 1). For Task 2, we will focus our effort on evaluating the hydrate formation time (Subtask 2.1) and computing the experimental uncertainty for the mass transfer coefficient (Subtask 2.3). We will provide a data table with the results of the hydrate formation time before September 30, 2017 as part of the success criteria for Decision Point 1. We will also submit a brief report documenting the success of our Matlab code for analyzing the NETL image data (Milestone 2, see Table 1). Following these activities, we will begin quantitative tracking of hydrate crystals on the bubble/water interface (Subtask 2.2) and analyze the mass transfer coefficient data to determine the correct form of the dissolution model (Eq. 1). Following this analysis, we will draft a journal article reporting our analysis of the mass transfer coefficient. Our target journal for this work is *Geochemistry, Geophysics, Geosystems.*

For Task 3, we will create a data table of all of the results of the image analysis (Subtask 3.1) and provide the data to NETL before September 30, 2017 as part of the success criteria for Decision Point 1. We will also prepare a brief report documenting our acoustic models (Milestone 3, see Table 1). Using this data, we will continue to draft a journal paper to report the results of the G08 cruise. Our target journal for this article is *Geophysical Research Letters.*

Table 1: Milestones schedule and verification methods.

	Milestone	Comments
Title	Acquisition of NETL HPWT data	
Date Completed	March 24, 2017	
Verification Method	Email verification	
Title	Adapt Matlab code to NETL data	
Planned Date	September 2017	
Verification Method	Report	
Title	Matlab code for M3 and EM-302 data	
Planned Date	September 2017	
Verification Method	Report	
Title	OTRC Experimental Report	
Planned Date	August 2018	
Verification Method	Report	
Title	Adapt seep model to NETL data	
Planned Date	June 2018	
Verification Method	Report	
Title	Quantify seep model performance	
Planned Date	December 2018	
Verification Method	Report	
Title	Quantify performance of acoustic models	
Planned Date	March 2019	
Verification Method	Report	

References

Clift, R., J. R. Grace, and M. E. Weber (1978), *Bubbles, drops, and particles*, Academic Press.

Fisher, H. B., E. J. List, R. C. Y. Koh, J. Imberger, and N. H. Brooks (1979), *Mixing in inland and coastal waters*, Academic Press.

Okubo, A. (1971), Oceanic diffusion diagrams, *Deep Sea Research and Oceanographic Abstracts*, *18*(8), 789–802.

Levine, J., I. Haljasmaa, R. Lynn, F. Shaffer, and R. P. Warzinski (2015), Detection of Hydrates on Gas Bubbles during a Subsea Oil/Gas Leak, NETL-TRS-6-2016, EPAct Technical Report Series, U.S. Department of Energy, National Energy Technology Laboratory: Pittsburgh, PA.

Rehder, G., I. Leifer, P. G. Brewer, G. Friederich, and E. T. Peltzer (2009), Controls on methane bubble dissolution inside and outside the hydrate stability field from open ocean field experiments and numerical modeling, *Marine Chemistry*, *114*(1-2), 19–30.

Wang, B., and S. A. Socolofsky (2015), A deep-sea, high-speed, stereoscopic imaging system for in situ measurement of natural seep bubble and droplet characteristics, *Deep Sea Research Part I*, *104*, 134–148.

Wang, B., S. A. Socolofsky, J. A. Breier, and J. S. Seewald (2016), Observation of bubbles in natural seep flares at MC 118 and GC 600 using in situ quantitative imaging, *Journal of Geophysical Research: Ocean*, *121*, 2203–2230.

Warzinski, R. P., F. Shaffer, R. Lynn, I. Haljasmaa, M. Schellhaas, B. J. Anderson, S. Velaga, I. Leifer, and J. Levine (2014), The role of gas hydrates during the release and transport of well fluids in the deep ocean, DOI/BSEE Contract E12PG00051/M11PPG00053, Final Report, U.S. Department of Energy, National Energy Technology Laboratory.

Warzinski, R. P., Lynn, R., Haljasmaa, I., Leifer, I., Shaffer, F., Anderson, B. J., and Levine, J. S. (2014). Dynamic morphology of gas hydrate on a methane bubble in water: Observations and new insights for hydrate film models. *Geophys Res Lett*, *41*(19), 2014GL061665.

Weber, T. C., L. Mayer, K. Jerram, J. Beaudoin, Y. Rzhanov, and D. Lovalvo (2014), Acoustic estimates of methane gas flux from the seabed in a 6000 km(2) region in the northern gulf of mexico, *Geochemistry Geophysics Geosystems*, *15*(5), 1911–1925.

2 Products

2.1 Publications, Conference Papers, and Presentations

Nothing to report

2.2 Websites or Other Internet Sites

The natural seep model used for this project, the Texas A&M Oilspill Calculator (TAMOC), is published via an open source code sharing service at:

http://github.com/socolofs/tamoc

2.3 Technologies or Techniques

Nothing to report.

2.4 Inventions, Patent Applications, and/or Licenses

Nothing to report.

2.5 Other Products

Nothing to report.

3 Participants and other collaborating organizations

3.1 Project Personnel

- 1. **Name**: Scott A. Socolofsky
  2. **Project Role**: Principal Investigator
  3. **Nearest person months worked during reporting period**: 1
  4. **Contribution to Project**: Overall project management and direction. Dr. Socolofsky has led the collection of the HPWT data, directed the data analysis methods, and completed all project reporting requirements.
  5. **Collaborated with individual in foreign country**: No
  6. **Travelled to foreign country**: No

- 1. **Name**: Binbin Wang
  2. **Project Role**: Co-Principal Investigator
  3. **Nearest person months worked during reporting period**: 2
  4. **Contribution to Project**: Analyzed the image data for the G08 cruise, created model for acoustic data from M3 sonar and EM-302 multibeam, and compared the measured data to model results from TAMOC. He also trained the Ph.D. student to begin analysis of the NETL HPWT data.
  5. **Collaborated with individual in foreign country**: No
  6. **Travelled to foreign country**: No

- 1. **Name**: Byungjin Kim
  2. **Project Role**: Ph.D. Student
  3. **Nearest person months worked during reporting period**: 3
  4. **Contribution to Project**: Organized the HPWT data, summarized the existing results from the NETL reports, and analyzed HPWT data for bubble size, hydrate formation time, and bubble interface mobility.
  5. **Collaborated with individual in foreign country**: No
  6. **Travelled to foreign country**: No

3.2 Partner Organizations

None to report.

3.3 External Collaborators or Contacts

This project works in close collaboration with researchers in the DOE/NETL funded project "Fate of Methane in the Water Column," led by the U.S. Geological Survey (USGS) in Woods Hole (Carolyn Ruppel), and with a new project led by the University of Rochester (John Kessler) to advance understanding of the environmental implications that methane leaking from dissociating gas hydrates could have on the ocean-atmosphere system. Dr. Socolofsky visits and communicates with researchers in these projects regularly and shares updates on work in progress. Accomplishments associated with these collaborations are detailed in Section 1.

4 Impact

None at this point.

5 Changes / Problems

Personnel. The project hired a Ph.D. Student beginning January 2017. This is a delay of three months from the original project plan. This delay occurred because the proposal for this project was written after the recruiting season for Ph.D. students for fall 2017 was already complete. This short delay of three months in starting a Ph.D. student on the project has not delayed performance in any of the current project tasks. We anticipate that we may request carry-forward of budgeted Ph.D. student salary and tuition at the end of Phase 1, and we may need to request a no-cost extension of up to three months at the end of the project.

6 Special Reporting Requirements

None required.

7 Budgetary Information

Table 2 summarizes expenditures for the current phase of the project. The current, reported spending is lower than actual because the co-PI, Binbin Wang, could not immediately be charged to the project. His title changed at Texas A&M University, which required written permission from the project manager at DOE NETL to bill his time. This approval was received, and we immediately submitted a payroll correction to move his salary charges to this project. However, because of the timing of the correction, the approval chain was not completed until early July, 2017. This payroll correction will be reflected in the Budget Report in the next reporting period. The remaining project spending will slightly lag the budget throughout Phase 1 due to the fact that the Ph.D. student was not hired in Q1, but rather started in Q2.

Table 2: Budget Report

Baseline Reporting Quarter DE-FE0028895	**Budget Period 1**							
	Q1 10/1/16 - 12/31/16		**Q2** 1/1/17 - 3/31/17		**Q3** 4/1/17 - 6/30/17		**Q4** 7/1/17 - 9/30/17	
	Q1	Cumulative Total	Q2	Cumulative Total	Q3	Cumulative Total	Q4	Cumulative Total
Baseline Cost Plan								
Federal Share	$33,752	$33,752	$29,716	$63,468	$27,810	$91,278	$53,034	$144,312
Non-Federal Share	$12,029	$12,029	$12,029	$24,058	$8,019	$32,077	$4,009	$36,086
Total Planned	$45,781	$45,781	$41,745	$87,526	$35,829	$123,355	$57,043	$180,398
Actual Incurred Cost								
Federal Share	$11,037	$11,037	$22,617	$33,654	$25,957	$ 59,610		
Non-Federal Share	$12,029	$12,029	$12,029	$24,058	$8,019	$ 32,077		
Total Incurred Costs	$23,066	$23,066	$34,646	$57,712	$33,976	$ 91,687		
Variance								
Federal Share	$-22,715	$-22,715	$-7,099	$-29,814	$-1,853	$-31,668		
Non-Federal Share	$0	$0	$0	$0	$0	$0		
Total Variance	$-22,715	$-22,715	$-7,099	$-29,814	$-1,853	$-31,668		